Breast Height Diameter Estimation From High-Density Airborne LiDAR Data

Alexander Bucksch, Roderik Lindenbergh, Muhammad Zulkarnain Abd Rahman, and Massimo Menenti

***Abstract*—High-density airborne light detection and ranging (LiDAR) data with point densities over 50 points/m^2 provide new opportunities, because previously inaccessible quantities of an individual tree can be derived directly from the data. We introduce a skeleton measurement methodology to extract the diameter at breast height (DBH) from airborne point clouds of trees. The estimates for the DBH are derived by analyzing the point distances to a suitable tree skeleton. The method is validated in three scenarios: 1) on a synthetic point cloud, simulating the point cloud acquisition over a forest; 2) on examples of free-standing and partly occluded trees; and 3) on automatically extracted trees from a sampled forest. The proposed diameter estimation performed well in all three scenarios, although influences of the tree extraction method and the field validation could not be fully excluded.**

***Index Terms*—Computational geometry, forestry, image analysis.**

I. Introduction

THE Actual Height model of The Netherlands (AHN2) [1] is a pioneering initiative to produce a detailed elevation model of a whole country. Such elevation information is highly demanded by water boards, provinces, and the national government. The elevation model utilizes high-density airborne laser altimetry, from which point clouds of individual objects are extractable. Skeletons are line-like descriptions that are established descriptors for shapes and have been applied to point clouds. Hence, linelike descriptions determined from such high-density airborne laser data and centered within the point cloud can be used to derive geometric measurements. In the context of this letter, we focus on the diameter at breast height (DBH) estimation of trees (stem diameter at 1.3 m height). In forestry, the DBH of individual trees is an important input parameter to estimate output parameters, such as the leaf area index [2], to obtain insight in the carbon water relations in forests [3] or into growth competition between individual trees [4]. Furthermore, the DBH is often used for hydrological applications because standing trees influence the water flow in flooded areas [5]. Many countries store the DBH of urban trees in cadastre databases for monitoring purposes. Except for urban trees, these applications have in common that no inventory of the detailed tree species exists. Available DBH estimation methods often incorporate species information as a variable, e.g., [6]. The importance of DBH for the estimation of the wooden tree volume is reported in [7]. Likewise, the same importance was mentioned in a comparison of high-density airborne- and terrestrial-obtained data to quantify individual trees [8].

Before estimating the DBH, the detection of individual trees from the data set is necessary, e.g., [9]–[16]. As a next step, allometric relations between crown size, tree height, and stem diameter are used to estimate the DBH [17]–[20] as a function of tree height and maximum crown width, incorporating species-dependent parameters [21]. An alternative to allometric approaches was first demonstrated by Monnet *et al.* [22], who used a supervised machine-learning approach to estimate forest stand parameters from sparse airborne data with 2.8 points/m^2 on average. In contrast to the method described in this letter, they estimated the mean diameter of a forest stand. The same machine-learning technique was used in [23] to derive individual stem diameters.

A skeleton-supported estimation of the DBH directly from the point cloud was only sketched in [24] and [25]. Previously, the SkelTre skeleton [26] was used to extract tree size parameters from terrestrial laser scanning data [27].

II. Methodology

A. Skeletonization of the Trees

Extracted individual trees serve as input to our method. Here, we used the method described in [28] to extract mature trees from a given data set. This particular method incorporates ground-level removal and filtering of understorey vegetation. The extracted trees are skeletonized with the SkelTre algorithm [26], which takes only one user-defined parameter as input. This parameter is the side length of cubes that initially subdivide the point cloud into unique equally sized volumes, each containing point-cloud points. From the point cloud of one tree (see Fig. 1, left), the 1-D SkelTre skeleton (see Fig. 1, middle) is derived. The SkelTre skeleton is a graph whose vertices are centered within the point cloud. The edges connecting the vertices describe the tree structure. A practical property of this skeleton is the correspondence between each vertex of the skeleton graph to a unique subset of points of the point cloud around the

Manuscript received July 31, 2013; revised September 17, 2013; accepted October 1, 2013. This work was supported by the Data ICT Dienst, Rijkswaterstaat, The Netherlands.

A. Bucksch was with the Department of Geoscience and Remote Sensing, Delft University of Technology, 2628 CN Delft, The Netherlands. He is now with the School of Interactive Computing, Georgia Institute of Technology, Atlanta, GA 30308 USA, and also with the School of Biology, Georgia Institute of Technology, Atlanta, GA 30332 USA (e-mail: bucksch@gatech.edu).

R. Lindenbergh and M. Menenti are with the Department of Geoscience and Remote Sensing, Delft University of Technology, 2628 CN Delft, The Netherlands.

M. Z. Abd Rahman was with the Department of Geoscience and Remote Sensing, Delft University of Technology, 2628 CN Delft, The Netherlands. He is now with the Department of Geoinformatics, Universiti Teknologi Malaysia, 81310 Johor Bahru, Johor, Malaysia.

Color versions of one or more of the figures in this paper are available online at http://ieeexplore.ieee.org.

Digital Object Identifier 10.1109/LGRS.2013.2285471

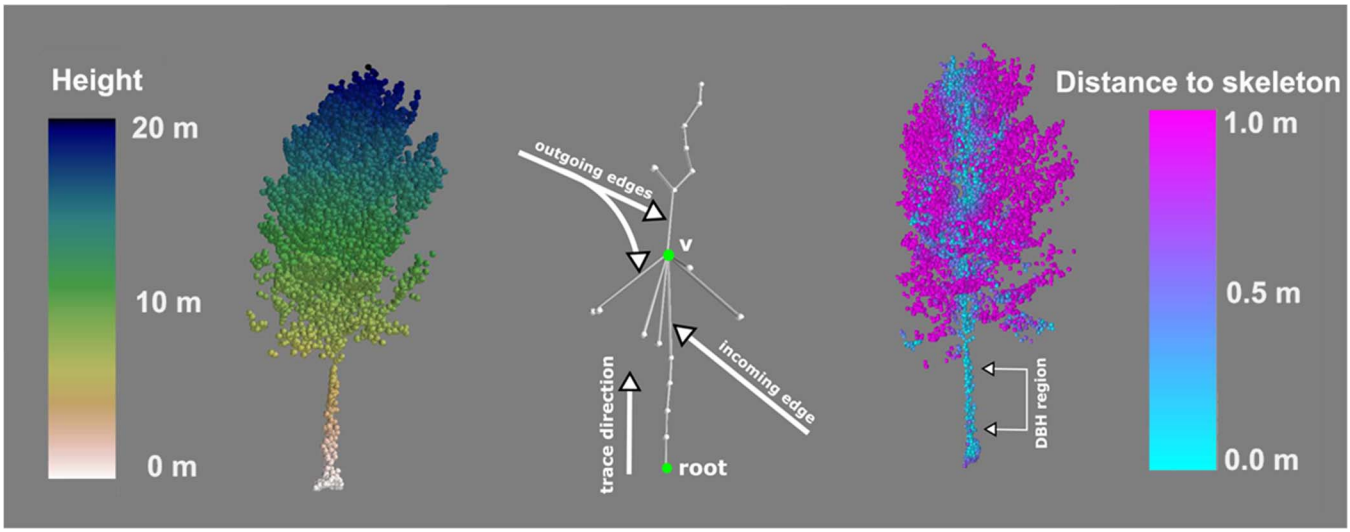

Fig. 1. Principle of the skeletonization. (Left) A tree point cloud obtained with high-density airborne laser scanning. The point cloud is colored by height. (Middle) SkelTre skeleton derived from the point cloud with 1.5-m minimum cell size. The stem is traced from the root vertex upward. v denotes the first vertex with more than two incident edges. (Right) Tree point cloud colored by distance to the calculated skeleton. The DBH region schematically marks the points used for calculating the DBH.

location of the vertex. In particular, the edge covering the breast height connects two vertices, which provides a point cloud subset suited for estimating the DBH. For details, we refer to [26].

B. Diameter Measurement

The diameter measurement is a three-step approach relying on the computation of the point-skeleton distance (see Fig. 1, right): first, the stem is extracted from the skeleton; second, a representative bin is chosen from the histogram of distances of the point-cloud points to the skeleton. This step results in a first estimation of the DBH. The reliability of this estimation is assessed in step 3, where an alternative geometrical construction is applied to detect a possible underestimation of the DBH in step 2.

Stem Extraction: The skeleton graph consists of vertices and edges (see Fig. 1, middle). The extraction of the stem from the skeleton graph follows a simple rule. The stem is extracted by tracing from the vertex representing the start of the stem at ground level (root vertex) upward. At each vertex, we evaluate the incoming and outgoing edges of the skeleton graph's vertices. An incoming edge is the last edge traced before reaching the vertex to be evaluated. All other edges are outgoing edges. In case of more than one outgoing edge, the edge forming an angle closest to 180° with the incoming edge is selected.

We select point-cloud points for obtaining the stem diameter by following the extracted stem from the root to the stem segment that covers the DBH. We assume that the diameter is not significantly varying between 1 and 4 m stem height for mature trees. This assumption allows us to add higher segments, until at least 40 points are collected or the 4-m height is reached to obtain a meaningful histogram of point-skeleton distances.

Histogram Evaluation: The distance $d(p)$ between each point-cloud point p belonging to the stem and the corresponding skeleton edge is computed as

$$d(p) = \frac{|(x_2 - x_1) \times (x_1 - p)|}{|x_2 - x_1|} \tag{1}$$

where d denotes the distance to a line defined by two points x_1 and x_2, which are the coordinates of the two vertices of an edge. Here, p denotes a point-cloud point, such that $z(x_1) \leq z(p) \leq z(x_2)$, where $z(.)$ denotes the z-coordinate.

From the calculated point-skeleton distances, a histogram is plotted. This histogram is calculated based on the assumption that every distance d represents the distance between the stem surface and the stem center. The majority of distances will result in a peak value in the histogram. The bin corresponding to the peak value is the so-called peak bin. If no unique peak bin exists, then the peak bin closest to the median of the distances is chosen for diameter evaluation. The mean d_H of the distances in the peak bin is assumed to be the estimate of the radius of the tree.

Validity Criterion: The motivation for a validity criterion is to enhance its robustness against diameter underestimations resulting from inaccurate centeredness of the skeleton graph. Inaccurate centeredness potentially leads to an underestimation of the diameter because of an increased amount of significantly smaller distances to the skeleton. Possible reasons for inaccurate centeredness are:

1) nonuniform sampling of the stem due to occlusion effects of neighboring trees and their canopies;
2) blunders in the sparse airborne data.

In the middle of a forest, the two situations are often amplified when trees are partly occluded from all sides.

This potential underestimation generated by occlusion effects and blunders motivates the evaluation of the estimated diameter d_H in four steps: First, the points at breast height used for estimating d_H are projected on a plane perpendicular to the local skeleton direction. As a second step, an approximation $d_Q = (1/(|Q|)) \sum_{i=1}^{|Q|} \max_{p \in Q} \|p - q_i\|$ of the outer diameter d_{outside} of the projected points is determined, where $Q = \{q_1, \ldots, q_{|Q|}\}$ is the set of all projected points (see supplemental material). The third step computes the threshold value $d_t = (1/2) d_Q \sqrt{3}$, to obtain an approximation of the

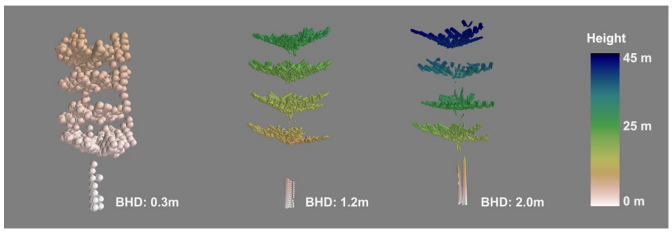

Fig. 2. FLI-MAP 400 simulation with 75 points/m^2. Three example trees from the simulation data set colored by height.

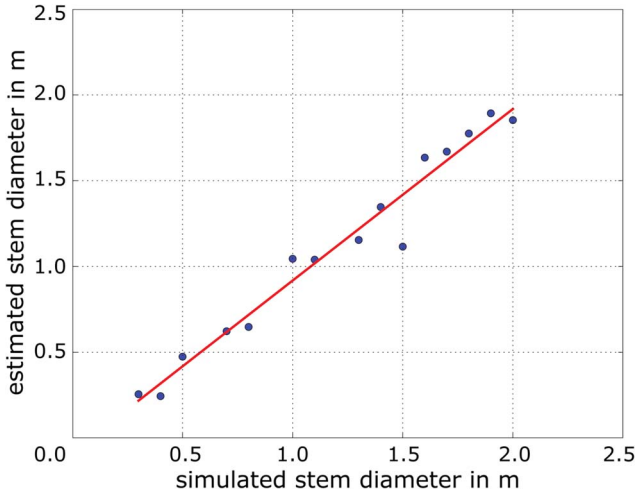

Fig. 3. Regression analysis of the DBH estimated for 18 test trees from the simulation data set. Three trees could not be analyzed with the histogram method and were excluded from the regression.

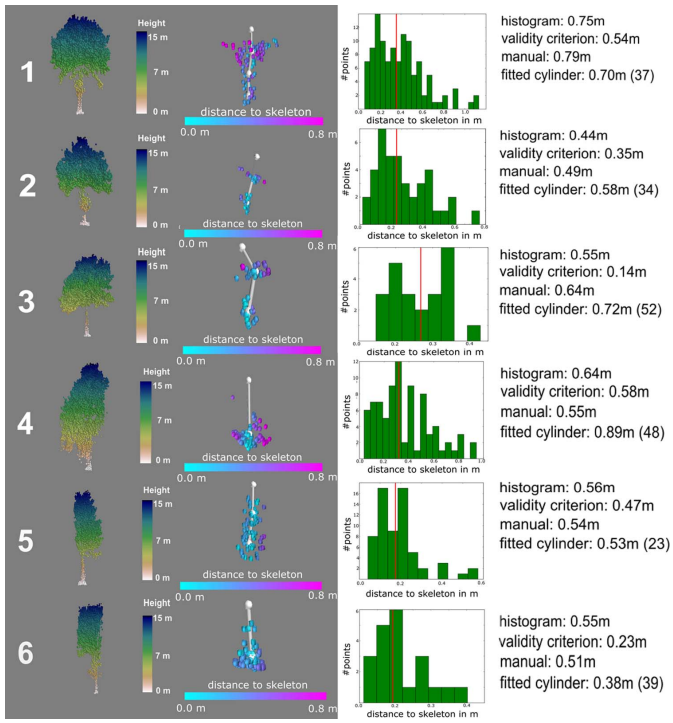

Fig. 4. Manually extracted trees. (Column 1) Input point cloud colored by height. (Column 2) Extracted skeleton and points used for diameter estimates. (Column 3) Histogram of the distances shows the median as a red vertical line. For every tree, the manual measurement, the diameter estimation with the histogram, the value of the validity criterion, and the diameter of a fitted cylinder with the number of points used in brackets are given.

inside diameter of the projected points, as given in [29]. If $d_H \leq d_t$, then d_t is taken, instead of d_H, as an estimation of the stem DBH.

III. Results and Validation

A. Simulated Data

The simulation data set used and its generation is described in detail in [30]. It simulates 75 points/m^2 measured from the top of an artificial forest patch. This forest patch contains 18 trees with diameters ranging equally in 0.1 m steps from 0.3 m to 2.0 m. The simulation data set is noise free, such that all projected stem points lie on a circle, but incorporates the effect of self-shadowing on the stem (see Fig. 2). Shadowing affected three of the 18 trees, such that less than 40 points were available to analyze. For the 15 remaining trees, a correlation coefficient of 0.97 and a root-mean-square error (RMSE) of the residuals to the regression line of 5 cm could be obtained (see Fig. 3). On the simulation data set, we used a minimum cell size of 2 m to extract a connected SkelTre skeleton and a histogram bin size of 5 cm. The validity criterion did not identify any poor estimates in this case.

B. Six Test Cases

Six FLI-MAP 400 point clouds sampling real trees were chosen to evaluate the histogram method (see Fig. 4). Trees 1–3 are free standing. Trees 4–6 are partly occluded trees from a forest border and, therefore, only partly sampled. Fig. 4 shows the point cloud colored by height, the extracted stem segment of the skeleton along with its corresponding points colored by point-skeleton distance, the histogram of point-skeleton distances, and the results of the diameter estimation for every tree. We give, in total, three measurements for each tree to facilitate the comparison: a manually obtained tape measurement as ground truth, the result obtained by the histogram method, and the diameter of a cylinder manually fitted to the stem points with the software Cyclone [31]. Additionally, the value of the validity criterion is reported. The six test cases were extracted by hand in order to eliminate the influence of the tree extraction method. We chose the smallest possible minimum cell size of 1.5 m that still resulted in a connected skeleton as input for the SkelTre algorithm. Tree 1 is considered as a standard case giving good results. Tree 2 is an example, where there are insufficient points present to estimate the diameter and noise is covering the middle of the stem. In case of Tree 3, the skeleton is attracted to one side because of the nonuniform sampling of the tree stem. A tree affected by shadowing effects (Tree 4) still gives an acceptable result (Tree 4), although the stem was covered by noise points. Observe here that insufficient removal of understorey vegetation as present on the base of the tree stem causes overestimation. Trees 5 and 6 again show good results close to the diameters observed in the field. In case of the six selected test cases, the data were of sufficient quality; therefore, the validity criterion was not necessary.

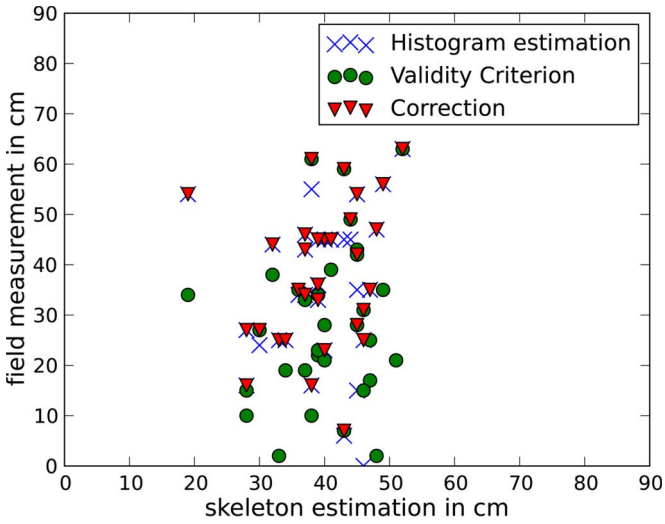

Fig. 5. Scatter plot of estimated and field-measured diameters. The mean/min/max errors are 16.4 cm/1.0 cm/46.0 cm for the histogram estimation, 12.6 cm/1.0 cm/46.0 cm for the validity criterion, and 11.6 cm/1.0 cm/36.0 cm after correction, respectively.

C. Extracted Trees From a Sampled Forest

A FLI-MAP 400 data set was collected over a mixed forest stand containing leaf and pine trees in the Duursche Waarde, The Netherlands. Forty-nine trees were extracted from the data set shown in Figs. 2 and 3 of the supplemental material. Depending on the chosen input parameters of the tree extraction algorithm, individual trees may be wrongly classified as understorey vegetation. On-site inspection of the forest patch revealed that five trees were not detected by the tree extraction method. From these 49 trees, one extracted tree was lying on the ground at the time of the field validation measurement, and one unresolvable case of a tree, which has grown two stems, was found. Only 34 were used for validation after filtering understorey vegetation. The manually measured average diameter of the 34 trees is 40 cm, showing a standard deviation of 7.2 cm with minimum and maximum diameters of 19 and 52 cm, respectively.

The histogram method without validity criterion resulted in an average diameter of 37 cm, which deviates only 3 cm from the manually obtained average diameter. The minimal diameter derived by the validity criterion shows an average of 28 cm. The validity criterion was active in six cases and improved the estimated average diameter to 39 cm. The diameter estimates derived with the histogram method, the lower bound diameters of the validity criterion, and the improved diameter estimates are shown in Fig. 5. Here, the largest avoided error by the validity criterion was 31 cm in the diameter. The diameters estimated with the histogram method show a standard deviation of 17 cm, whereas the lower bound diameters detected by the validity criterion show a standard deviation of 15 cm. Applying the validity criterion slightly improved the original standard deviation of the histogram method to 16 cm. Only the combined use of the histogram method and the validity criterion resulted in a significant but weak correlation ($r^2 = 0.11$, $p < 0.1$, spearman $r = 0.36$, $p < 0.05$). We calculated the RMSE for the data shown in Fig. 5 as RMSE $= \sqrt{\sum_{i=0}^{n}(c_i - f_i)^2}$, where n is the number of measured trees, c are the computed diameters, and f are the field-measured diameters. The RMSE resulted in 2.6 cm (6.8%) for the data improved with the validity criterion, in 3.0 cm (8.1%) for the histogram estimation, and in 3.4 cm (12.2%) for the minimal diameters derived by the validity criterion alone. The mean/min/max errors are 16.4 cm/1.0 cm/46.0 cm for the histogram estimation, 12.6 cm/1.0 cm/46.0 cm for the validity criterion, and 11.6 cm/1.0 cm/36.0 cm after correction, respectively. We found that the extracted trees in the interior of the forest were affected by strong underestimations. Here, we again used a minimum cell size of 1.5 m as input to the skeletonization algorithm.

IV. Discussion and Conclusion

We have presented a new promising DBH estimation concept and introduced an upper bound to avoid overestimations. For deciduous forests, the method is restricted to leaf-off conditions to obtain a significant amount of laser pulse returns from the tree stems. For applications focusing on free-standing trees, such as those shown in the six test cases, insufficient stem sampling was not an observed issue. In summer, with a dense leaf roof where almost no pulse returns from the stem are obtainable, traditional allometric methods are favorable because tree crown width and height are still possible to estimate. Another problem is the removal of understorey vegetation, which can cause the unwanted removal of data points belonging to the stem. Removed data points might be the reason for observed underestimations compared to the manual ground truth. The amount of pulse returns on the tree stem currently limits the method, such that up to 4 m of the stem length are used for the DBH estimation. Fortunately, increasing data density will lower the stem threshold. To date, 170 points/m^2 have been already reported [32]. A future validation strategy is to estimate the DBH from repeated light detection and ranging (LiDAR) data of the same forest patch. The variation in outcome will give more insight in the robustness of the presented method, since the DBH is not expected to change significantly in one year for full-grown trees.

The main advantage of our method is the ability to compute the DBH for individual trees directly from the point cloud. The difficulties to relocate individual trees in a complex forest impede the collection of a large validation data set, because the dense canopy does not allow precise GPS locations to obtain reliable tree positions. Future research has to detail the influence of the tree extraction process and the understorey filtering to enable automatic estimations in real forest scenarios. Nevertheless, results from the simulated trees and from the six individual trees give enough evidence to conclude that skeletonization of trees is feasible for high-density airborne data. It is predictable that data of even higher density will be widely available in the near future, which positively influences the performance of already-known tree extraction algorithms and the quality of the skeletonization. Overall, high-density airborne data enable the extraction of parameters on an individual tree level. Initial studies indicate that tree inclination and orientation will be robustly derived [33]. Such information is not accessible through low-density data that do not contain information about the stem

geometry. Nevertheless, high-density airborne data imply the cost of more data and the need for even more computation resources.

REFERENCES

[1] L. Swart, "How the up-to-date height model of The Netherlands (AHN) became a massive point data cloud," in *Proc. Manage. Massive Point Cloud Data: Wet and Dry*, 2010, pp. 1–18, Nederlandse Commissie voor Geodesie.

[2] I. Jonckheere, S. Fleck, K. Nackaerts, B. Muys, C. P. M. Weiss, and F. Baret, "A review of methods for leaf area index estimation of forest stands focused on digital hemispherical photography," *Agr. Forest Meteorol.*, vol. 121, no. 1, pp. 19–35, 2004.

[3] B. Köstner, M. Schmidt, E. Falge, S. Fleck, and J. D. Tenhunen, "Atmospheric and structural controls on carbon and water relations in mixed-forest stands," in *Temperate Forest Ecosystems Response to Changing Environment: Watershed Studies in Germany*, E. Matzner, Ed. Berlin, Germany: Springer-Verlag, 2004, pp. 69–98.

[4] C.-S. Lo and C. Lin, "Growth-competition-based stem diameter and volume modeling for tree-level forest inventory using airborne LiDAR data," *IEEE Trans. Geosci. Remote Sens.*, vol. 51, no. 4, pp. 2216–2226, Apr. 2013.

[5] M. W. Straatsma and M. J. Baptist, "Floodplain roughness parameterization using airborne laser scanning and spectral remote sensing," *Remote Sens. Environ.*, vol. 112, no. 3, pp. 1062–1080, Mar. 2008.

[6] T. Takahashi, K. Yamamoto, Y. Senda, and M. Tsuzuku, "Predicting individual stem volumes of sugi (*Cryptomeria japonica D. Don*) plantations in mountainous areas using small-footprint airborne LiDAR," *J. Forest Res.*, vol. 10, no. 4, pp. 305–312, Aug. 2005.

[7] C. Edson and M. G. Wing, "Airborne light detection and ranging (LiDAR) for individual tree stem location, height, and biomass measurements," *Remote Sens.*, vol. 3, no. 11, pp. 2494–2528, Nov. 2011.

[8] S.-E. Jung, D.-A. Kwak, T. Park, W.-K. Lee, and S. Yoo, "Estimating crown variables of individual trees using airborne and terrestrial laser scanners," *Remote Sens.*, vol. 3, no. 11, pp. 2494–2528, Oct. 2011.

[9] C. Meia and S. Durrieu, "Tree crown delineation from digital elevation models and high resolution imagery," in *Proc. IAPRS*, 2004, vol. 36, pp. 218–223.

[10] E. Naesset and T. Okland, "Estimating tree height and tree crown properties using airborne scanning laser in a boreal nature reserve," *Remote Sens. Environ.*, vol. 79, no. 1, pp. 105–115, Jan. 2002.

[11] S. C. Popescu, R. H. Wynne, and R. F. Nelson, "Measuring individual tree crown diameter with LiDAR and assessing its influence on estimating forest volume and biomass," *Can. J. Remote Sens.*, vol. 29, no. 5, pp. 564–577, Oct. 2003.

[12] H. Kaartinen, J. Hyyppä, X. Yu, M. Vastaranta, H. Hyyppä, A. Kukko, M. Holopainen, C. Heipke, M. Hirschmugl, F. Morsdorf, E. Nsset, J. Pitknen, S. Popescu, S. Solberg, B. Wolf, and J. Wu, "An international comparison of individual tree detection and extraction using airborne laser scanning," *Remote Sens.*, vol. 4, no. 4, pp. 950–974, Mar. 2012.

[13] J. Vauhkonen, L. Ene, S. Gupta, J. Heinzel, J. Holmgren, J. Pitknen, S. Solberg, Y. Wang, H. Weinacker, and K. Hauglin, "Comparative testing of single-tree detection algorithms under different types of forest," *Forestry*, vol. 85, no. 1, pp. 27–40, Jan. 2012.

[14] J. Hyyppä, T. Mielonen, H. Hyyppä, M. Maltamo, X. Yu, E. Honkavaara, and H. Kaartinen, "Using individual tree crown approach for forest volume extraction with aerial images and laser point clouds," in *IARPS*, 2005, vol. 36, no. 3, pp. 144–149.

[15] J. Kalliovirta and T. Tokola, "Functions for estimating stem diameter and tree age using tree height, crown width and existing stand database information," *Silva Fennica*, vol. 39, no. 2, pp. 227–248, 2005.

[16] X. Yu, J. Hyyppä, M. Vastaranta, M. Holopainen, and R. Viitala, "Predicting individual tree attributes from airborne laser point clouds based on the random forests technique," *ISPRS J. Photogramm. Remote Sens.*, vol. 66, no. 1, pp. 28–37, Jan. 2011.

[17] H. E. Andersen, S. E. Reutebuch, and R. J. McGaughey, "A rigorous assessment of tree height measurements obtained using airborne LiDAR and conventional field methods," *Can. J. Remote Sens.*, vol. 32, no. 5, pp. 355–366, Oct. 2006.

[18] H. Buddenbaum and S. Seeling, "Derivation of tree height and crown closure from airborne LiDAR imagery," *Geophys. Res. Abstracts*, vol. 9, pp. 322–336, 2007.

[19] M. L. Clark, D. B. Clark, and D. A. Roberts, "Small-footprint LiDAR estimation of sub-canopy elevation and tree height in a tropical rain forest landscape," *Remote Sens. Environ.*, vol. 91, no. 1, pp. 68–89, May 2004.

[20] I. Korpela, B. Dahlin, H. Schäfer, E. Bruun, F. Haapaniemi, J. Honkasalo, S. Ilvesniemi, V. Kuutti, M. Linkosalmi, J. Mustonen, M. Salo, O. Suomi, and H. Virtanen, "Single-tree forest inventory using LiDAR and aerial images for 3D treetop positioning, species recognition, height and crown width estimation," in *Proc. IAPRS*, 2007, vol. 36, no. 3, pp. 227–233.

[21] J. Laasasenaho, "Taper curve and volume functions for pine, spruce and birch," *Commun. Inst. Forestalls Fenniae*, no. 108, pp. 1–74, 1982.

[22] J.-M. Monnet, J. Chanussot, and F. Berger, "Support vector regression for the estimation of forest stand parameters using airborne laser scanning," *IEEE Geosci. Remote Sens. Lett.*, vol. 8, no. 3, pp. 580–584, May 2011.

[23] M. Dalponte, L. Bruzzone, and D. Gianelle, "A system for the estimation of single-tree stem diameter and volume using multireturn LiDAR data," *IEEE Trans. Geosci. Remote Sens.*, vol. 49, no. 7, pp. 2479–2490, Jul. 2011.

[24] A. Bucksch, R. Lindenbergh, M. Menenti, and M. Z. Rahman, "Skeleton-based botanic tree diameter estimation from dense LiDAR data," in *Proc. SPIE*, Bellingham, WA, USA, 2009, vol. 7460, pp. 746 007-1–746 007-11.

[25] M. Z. Rahman, B. Gorte, and A. Bucksch, "A new method for individual tree measurement from airborne LiDAR," in *Proc. SilviLaser*, College Station, TX, USA, 2009, pp. 14–16.

[26] A. Bucksch, R. Lindenbergh, and M. Menenti, "SkelTre—Robust skeleton extraction from imperfect point clouds," *Visual Comput.*, vol. 26, no. 10, pp. 1283–1300, Oct. 2010.

[27] A. Bucksch and S. Fleck, "Automated detection of branch dimensions in woody skeletons of fruit tree canopies," *Photogramm. Eng. Rem. S*, vol. 77, no. 3, pp. 229–240, Mar. 2011.

[28] M. Z. Rahman, B. Gorte, and A. Bucksch, "A new method for individual tree delineation and undergrowth removal from high resolution airborne LiDAR," in *Proc. IARPS*, 2009, vol. 38, no. 3, pp. 283–288.

[29] M. Löffler and M. van Kreveld, "Largest bounding box, smallest diameter, and related problems on imprecise points," *Comput. Geometry*, vol. 43, no. 4, pp. 419–433, May 2010.

[30] M. Rahman, "Estimation of composite hydrodynamic roughness over land with high density airborne laser scanning," Ph.D. dissertation, Delft Univ. Technol., Delft, The Netherlands, 2011.

[31] Leica Geosystems, Aarau, Switzerland, "Software: Cyclone 6.0," 3D Point Cloud Processing Software 2009.

[32] K. A. Razak, A. Bucksch, M. Straatsma, C. J. Van Westen, R. A. Bakar, and S. M. de Jong, "High density airborne LIDAR estimation of disrupted trees induced by landslides," in *Proc. IEEE Int. Geosci. Remote Sens. Symp.*, Melbourne, Australia, 2013, pp. 2617–2620.

[33] K. A. Razak, A. Bucksch, M. Damen, C. van Westen, M. Straatsma, and S. de Jong, "Characterizing tree growth anomaly induced by landslides using LiDAR," in *Proc. 2nd World Landslide Forum*, Rome, Italy, 2011, pp. 235–241.